Interleukins 4 and 13 drive lipid abnormalities in skin cells through regulation of sex steroid hormone synthesis

Chenlu Zhang[a,1], Mahendran Chinnappan[a,1], Courtney A. Prestwood[a], Marshall Edwards[a], Methinee Artami[a], Bonne M. Thompson[b], Kaitlyn M. Eckert[b], Goncalo Vale[b,c], Christos C. Zouboulis[d], Jeffrey G. McDonald[b,c], and Tamia A. Harris-Tryon[a,e,2]

[a]Department of Dermatology, University of Texas Southwestern Medical Center, Dallas, TX 75390; [b]Center for Human Nutrition, University of Texas Southwestern Medical Center, Dallas, TX 75390; [c]Department of Molecular Genetics, University of Texas Southwestern Medical Center, Dallas, TX 75390; [d]Department of Dermatology, Venereology, Allergology and Immunology, Dessau Medical Center, Brandenburg Medical School Theodore Fontane and Faculty of Health Sciences Brandenburg, 06847 Dessau, Germany; and [e]Department of Immunology, University of Texas Southwestern Medical Center, Dallas, TX 75390

Edited by John J. O'Shea, NIH, Bethesda, MD, and accepted by Editorial Board Member Tadatsugu Taniguchi July 12, 2021 (received for review January 16, 2021)

Atopic dermatitis (AD) is a chronic inflammatory skin disease characterized by skin dryness, inflammation, and itch. A major hallmark of AD is an elevation of the immune cytokines IL-4 and IL-13. These cytokines lead to skin barrier disruption and lipid abnormalities in AD, yet the underlying mechanisms are unclear. Sebaceous glands are specialized sebum-producing epithelial cells that promote skin barrier function by releasing lipids and antimicrobial proteins to the skin surface. Here, we show that in AD, IL-4 and IL-13 stimulate the expression of 3β-hydroxysteroid dehydrogenase 1 (HSD3B1), a key rate-limiting enzyme in sex steroid hormone synthesis, predominantly expressed by sebaceous glands in human skin. HSD3B1 enhances androgen production in sebocytes, and IL-4 and IL-13 drive lipid abnormalities in human sebocytes and keratinocytes through HSD3B1. Consistent with our findings in cells, HSD3B1 expression is elevated in the skin of AD patients and can be restored by treatment with the IL-4Rα monoclonal antibody, Dupilumab. Androgens are also elevated in a mouse model of AD, though the mechanism in mice remains unclear. Our findings illuminate a connection between type 2 immunity and sex steroid hormone synthesis in the skin and suggest that abnormalities in sex steroid hormone synthesis may underlie the disrupted skin barrier in AD. Furthermore, targeting sex steroid hormone synthesis pathways may be a therapeutic avenue to restoring normal skin barrier function in AD patients.

androgens | atopic dermatitis | sebaceous glands | skin lipids | Dupilumab

Atopic dermatitis (AD) is a chronic inflammatory skin disease characterized by stratum corneum lipid abnormalities (1, 2) and a dysfunctional skin barrier (3). The skin is a vital organ separating the host from its environment, and thus, the barrier breakdown seen in AD has systemic consequences for the host. AD patients experience more frequent episodes of skin infection from the increased exposure to commensal microbes. Additionally, the deeper penetration of environmental allergens in AD skin promotes the sequential progression of AD to other atopic diseases, including allergic rhinitis, food allergy, and asthma (4). AD is also an increasingly common condition with up to 13% of children and 10% of adults suffering from AD, with an annual treatment cost of $5.3 billion in the United States alone (5, 6).

A major hallmark of AD is the elevated production of interleukins 4 and 13 (IL-4 and IL-13), both type 2 cytokines. These cytokines are pathogenic and drive the inflammation and barrier disruption seen in AD (7). Dupilumab is a human monoclonal antibody directed against the shared alpha subunit of the IL-4 and IL-13 receptors (IL-4Rα) and has revolutionized therapy for patients with moderate to severe AD and asthma (8). It is clear that blockade of IL-4Rα signaling restores skin barrier function and skin lipid metabolism in AD patients (9–11); however; how these classical immune pathways impact the skin epithelium is less clearly defined.

Sebaceous glands are composed of specialized epithelial cells called sebocytes that generate sebum—a unique oily mixture of wax esters, squalene, triglycerides, proteins, and fatty acids required for normal skin ecology (12–15). Sebum is essential for barrier function, yet few current studies have examined the impact of sebaceous glands in the pathogenesis of AD (3, 11, 16, 17). Here, we explore how human sebocytes respond to the cytokines IL-4 and IL-13 to begin to establish how these cells impact barrier dysfunction in AD. We show that IL-4 and IL-13 upregulate the expression of 3β-hydroxysteroid dehydrogenase 1 (HSD3B1) in sebaceous glands through the activation of STAT6. HSD3B1 is the rate-limiting enzyme in the synthesis of all classes of steroid hormones in primates (18, 19). Thus, IL-4 and IL-13 stimulate the production of the sex steroids androstenedione and dihydrotestosterone in sebocytes. Consistent with our findings in culture, the expression of HSD3B1 is also highly elevated in the lesional skin of human AD patients, which can be restored by Dupilumab treatment. Furthermore, we utilized small interfering RNA (siRNA) targeting HSD3B1 and show that depletion of

Significance

Atopic dermatitis (AD) is a chronic inflammatory skin condition affecting 13% of adults and 10% of children worldwide. The inflammation seen in AD is driven by type 2 cytokines, including IL-4 and IL-13. We have an incomplete understanding about how these cytokines impact the epithelial barrier and drive AD pathology. Our study demonstrates that IL-4 and IL-13 promote androgen production and drive lipid abnormalities in sebocytes. These findings deepen our understanding of the impact of the immune system on the skin epithelium.

Author contributions: C.Z., M.C., J.G.M., and T.A.H.-T. designed research; C.Z., M.C., C.A.P., M.E., M.A., B.M.T., K.M.E., G.V., and T.A.H.-T. performed research; C.C.Z. contributed new reagents/analytic tools; C.Z., B.M.T., K.M.E., G.V., J.G.M., and T.A.H.-T. analyzed data; C.Z., K.M.E., and T.A.H.-T. wrote the paper; and C.C.Z. edited the manuscript.

The authors declare no competing interest.

This article is a PNAS Direct Submission. J.J.O. is a guest editor invited by the Editorial Board.

[1]C.Z. and M.C. contributed equally to this work.

[2]To whom correspondence may be addressed. Email: tamia.harris-tryon@utsouthwestern.edu.

This article contains supporting information online at https://www.pnas.org/lookup/suppl/doi:10.1073/pnas.2100749118/-/DCSupplemental.

Published September 14, 2021.

HSD3B1-derived sex steroids in sebocytes increases lipid synthesis machinery in sebocytes and keratinocytes. Current treatments for AD primarily focus on immunosuppression to combat type 2 inflammation (20). Our findings provide insight into the impact of type 2 cytokines on skin ecology and uncover the sex steroid hormone synthesis pathway as a potential therapeutic target for the treatment of AD in humans.

Results

IL-4 and IL-13 Induce HSD3B1 Expression in Human Sebaceous Gland Cells. To investigate the role of sebaceous gland cells in AD pathogenesis, we began by studying the immortalized human sebaceous gland cell line SZ95 (21). SZ95 cells were treated with 10 ng/mL of IL-4 and IL-13 for 24 h, and the whole transcriptome was analyzed by RNA-sequencing (RNA-seq) (*SI Appendix*, Fig. S1*A* and Dataset S1). The RNA-seq data revealed a total of 61 differentially expressed genes (DEGs) with fold change >1.8 and adjusted *P* value <0.01 in treated SZ95 cells as compared with untreated controls (Fig. 1*A*). Among those DEGs, there are 56 genes showing increased expression with IL-4 and IL-13 treatment. Gene ontology enrichment analysis revealed that genes involved in ion transport, response to virus, and oxidation-reduction processes were enriched in these up-regulated genes (*SI Appendix*, Fig. S1*B*).

The most pronounced response of SZ95 cells to IL-4 and IL-13 was an increase in the messenger RNA of *HSD3B1* (Fig. 1*A* and *SI Appendix*, Fig. S1*C*). *HSD3B1* encodes an enzyme that catalyzes the oxidative conversion of hydroxysteroid precursors into ketosteroids, a critical and rate-limiting step in the production of all classes of steroid hormones (*SI Appendix*, Fig. S2). To confirm that HSD3B1 expression is induced by IL-4 and IL-13 in SZ95 cells, we used Western blots to analyze the change in HSD3B1 protein expression in SZ95 cells treated with cytokines. Consistent with our RNA-seq results, HSD3B1 protein expression increased after IL-4 and IL-13 treatment in SZ95 cells (Fig. 1*B*). Furthermore, qRT-PCR of IL-4 and IL-13–treated SZ95 cells displayed a 60- to 100-fold increase in the relative expression of *HSD3B1* compared to untreated cells (Fig. 1*C* and *SI Appendix*, Fig. S1*D*). There was no difference in *HSD3B1* expression when SZ95 cells were treated with other cytokines, including the type-2 cytokines IL-5 and IL-33, the antiviral cytokine interferon (IFN)-γ, or IL-17α and IL-23 (Fig. 1*C* and *SI Appendix*, Fig. S1*D*), indicating a specific response of *HSD3B1* to IL-4 and IL-13. Interestingly, the expression of cytochrome P450 family 11 subfamily A member 1 (*CYP11A1*), another gene involved in the synthesis of steroid hormones, was also up-regulated by IL-4 and IL-13 in the SZ95 cells (Fig. 1*A* and *SI Appendix*, Fig. S1*C*). CYP11A1 catalyzes the conversion of cholesterol to pregnenolone through side-chain cleavage (*SI Appendix*, Fig. S2).

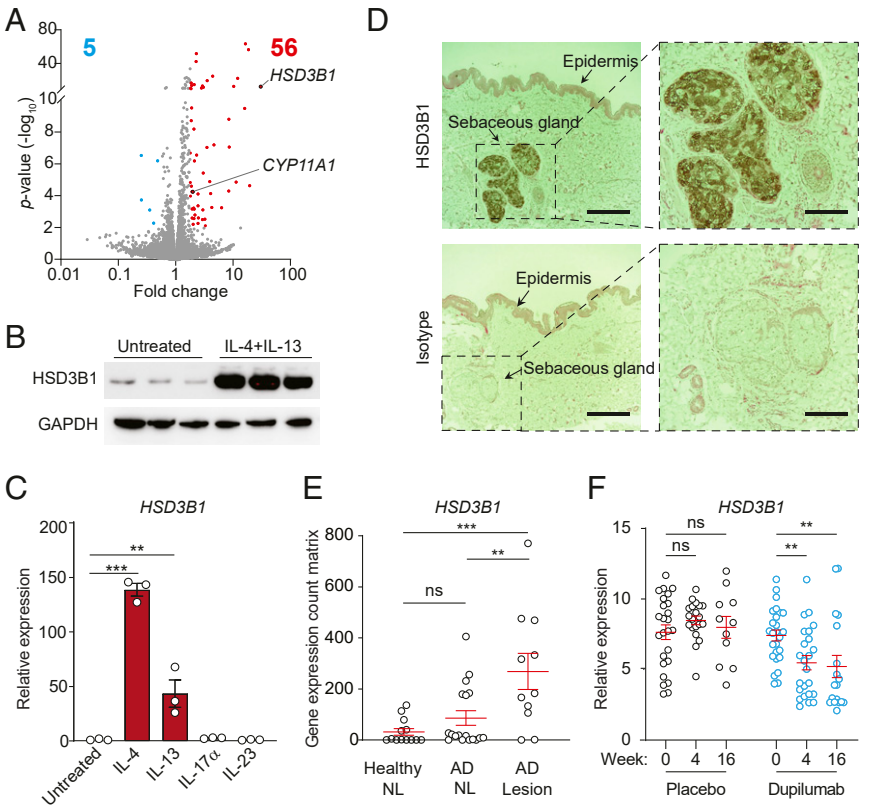

Fig. 1. The expression of HSD3B1 is induced by IL-4 and IL-13 cytokines in atopic skin and human sebocytes. (*A*) Volcano plot with significantly DEGs (fold change >1.8 and $P < 0.01$) highlighted in red (up-regulated in IL-4 and IL-13 treated) and blue (down-regulated in IL-4 and IL-13 treated). (*B*) Western blot analysis of HSD3B1 was performed on untreated or IL-4- and IL-13-treated SZ95 cells. GAPDH was used as the loading control. (*C*) RT-qPCR analysis of *HSD3B1* transcript in the untreated- and various cytokine-treated human SZ95 sebocytes. (*D*) Immunohistochemistry detection of HSD3B1 in human skin. IgG isotype staining as negative control. Epidermis and sebaceous gland indicated with an arrow. (*Left* scale bar, 500 μm.) (*Right* scale bar, 200 μm.) (*E*) We analyzed the publicly available RNA-seq dataset of skin tape strip RNA samples (11). Transcript abundances of *HSD3B1* in human skin as detected by RNA-seq analysis of skin tape strip RNA samples collected from healthy individual nonlesions (NL) and AD patients' NL and lesions. Healthy NL skin ($n = 13$), AD NL skin ($n = 18$), and AD lesional skin ($n = 11$). (*F*) Analysis of publicly available microarray dataset (25). *HSD3B1* transcript abundance in AD patient skin after 4 or 16 wk of Dupilumab (blue) or placebo (black) treatment compared to baseline, week 0. Means ± SEM are plotted, $^{**}P < 0.01$, $^{***}P < 0.001$, ns (not significant) was determined by one-way ANOVA.

SZ95 cells are derived from the face of an elderly female patient (21). As *HSD3B1* and *CYP11A1* are genes involved in sex steroid hormone synthesis that might display differential expression in male skin, we also completed parallel studies in SEB-1 cells—a second immortalized human sebaceous gland cell line derived from the preauricular skin of a male patient (22). Congruent with our findings in female-derived cells, *HSD3B1* and *CYP11A1* expression are also markedly up-regulated by IL-4 and IL-13 treatment in SEB-1 cells (*SI Appendix*, Fig. S1*E*). Together, these data reveal that the expression of genes involved in the steroid hormone synthesis pathway, especially HSD3B1, are highly up-regulated by IL-4 and IL-13 in immortalized human sebaceous gland cells.

Next, using an antibody specific for HSD3B1 we investigated the expression pattern of HSD3B1 protein in skin by both immunohistochemistry (Fig. 1*D*) and immunofluorescence (*SI Appendix*, Fig. S3*A*). In healthy skin, cells outside of the sebaceous gland, including keratinocytes and the dermal papillae, were negative for HSD3B1 protein expression (Fig. 1*D*). Previous studies on immortalized keratinocytes showed that HaCaT cells can produce *HSD3B1* transcript upon stimulation with IL-4 and IL-13 (23). Thus, we further investigated the protein expression of HSD3B1 (*SI Appendix*, Fig. S3*C*). Indeed, HaCaT cells do produce HSD3B1 protein in culture upon stimulation with IL-4 and IL-13 (*SI Appendix*, Fig. S3*C*). However, the stimulated expression of HSD3B1 protein in keratinocytes is less marked than the expression in sebocytes at baseline and after stimulation by IL-4 and IL-13 (*SI Appendix*, Fig. S3*C*). Lastly, we completed immunohistochemistry on AD skin (*SI Appendix*, Fig. S3*B*). Similar to what we observed in normal skin (Fig. 1*D*), HSD3B1 is expressed in the sebaceous gland of AD skin, with low expression of HSD3B1 protein in the epidermis (*SI Appendix*, Fig. S3*B*). In aggregate, these data confirm that HSD3B1 is a sebaceous gland predominant enzyme in vivo (24), up-regulated by IL-4 and IL-13 in epithelial cells.

HSD3B1 Expression Is Increased in the Skin of AD Patients. To determine if our findings in vitro were relevant for AD skin, we analyzed a publicly available RNA-seq dataset from a previously published study (11). This dataset contained skin tape strip samples from 11 adults of European descent with active AD and 13 nonatopic healthy individuals with no family history of atopic skin diseases (*SI Appendix*, Fig. S4*A*). Compared to the skin of healthy control individuals, AD lesional skin displayed a characteristic AD-associated transcriptomic profile, including the increased expression of related cytokines, chemokines, and skin barrier proteins (*SI Appendix*, Fig. S4*B*). Consistent with our findings in SZ95 cells, the *HSD3B1* transcript is more abundant in AD lesional skin compared to the skin of healthy controls (Fig. 1*E*). Notably, the expression level of *HSD3B1* is also higher in AD lesional skin compared to nonlesional skin of AD patients (Fig. 1*E*), suggesting that the local environment in AD drives the increased expression of *HSD3B1* in the skin of AD patients. Next, we explored changes of transcript abundance of genes involved more broadly in sex steroid hormone biosynthesis and metabolism (*SI Appendix*, Fig. S4*C*). The expression of *SRD5A3* (steroid 5 alpha-reductase 3), *HSD17B12* (hydroxysteroid 17-beta dehydrogenase 12), *SULT2B1* (sulfotransferase family 2B member 1), and *UGT1A7* (UDP glucuronosyltransferase family 1 member A7), which are involved in the synthesis or metabolism of sex steroid hormones, are also increased in AD lesional skin samples. These findings suggest that local sex steroid hormone metabolism in AD lesional skin might be disrupted.

To further explore the impact of the immune system on *HSD3B1* expression, we assessed how treatment of atopic skin with the monoclonal antibody, Dupilumab, affected *HSD3B1* expression. We analyzed *HSD3B1* transcript abundance in a microarray dataset of skin punch biopsy samples from AD patients treated with placebo or Dupilumab, for up to 16 wk (25). Notably, after 4 wk or 16 wk of Dupilumab treatment, *HSD3B1* expression is significantly reduced (Fig. 1*F*). Taken together, these findings from independent patient datasets suggest that *HSD3B1* is regulated by IL-4 and IL-13 in AD skin.

STAT6 Activates HSD3B1 Transcription by Binding Directly to Its Promoter. We next sought to examine the signaling pathway that regulates the expression of *HSD3B1* in sebocytes. The transcription factor STAT6 (signal transducer and activator of transcription 6) is a key response element downstream of the IL-4 receptor (IL-4R). Activation of IL-4R leads to phosphorylation of STAT6, which then binds to the promoters of its target genes and activates their transcription. Western blot analysis of total cell protein extracts using a specific anti–P-STAT6 (Tyr-641) antibody shows that addition of IL-4 and IL-13 results in STAT6 phosphorylation in sebocytes. Similar amounts of total STAT6 were also detected as an input control (Fig. 2 *A* and *B*).

Furthermore, examination of the *HSD3B1* gene promoter sequence suggested that STAT6 could be directly mediating regulation of the *HSD3B1* promoter. The sequence TTCCTGGGAA at −267 to −258 is the predicted STAT6 binding site that matches to the consensus palindromic core motif $TTCN_4GAA$ for human STAT6 (Fig. 2*C*). Electrophoretic Mobility Shift Assays were used to further confirm the direct interaction between phosphorylated STAT6 (pSTAT6) protein and a target DNA sequence in the HSD3B1 promoter. Unphosphorylated human STAT6 core fragment ($STAT6^{CF}$, amino acids 123 to 658) was expressed in *Escherichia coli* (*SI Appendix*, Fig. S5 *A–C*). We generated phosphorylated $STAT6^{CF}$ protein by coexpressing $STAT6^{CF}$ with an inducible tyrosine kinase gene (pTK) contained in the bacterial strain (*SI Appendix*, Fig. S5 *D–F*) and confirming their expression by Western blot analysis (Fig. 2*D*). Purified $STAT6^{CF}$ or $pSTAT6^{CF}$ protein was mixed with different stretches of DNA amplified by PCR of the *HSD3B1* promoter. Only complexes of phosphorylated $STAT6^{CF}$ and the (−300 to 0) DNA fragment showed hindered movement in a 6% polyacrylamide DNA retardation gel (see Fig. 2*E* and *SI Appendix*, Fig. S5*G*). The DNA fragment (−258 to 0) without the predicted binding site was unable to bind $pSTAT6^{CF}$ protein (see Fig. 2*E*). Additionally, knockdown of STAT6 with siRNAs decreased the stimulated expression of *HSD3B1* in sebocytes (Fig. 2*F*). Taken together, these findings demonstrate that STAT6 is a transcriptional activator of *HSD3B1* in sebocytes, through direct binding to the promoter at the predicted binding sequence.

IL-4 and IL-13 Promote HSD3B1-Dependent Androgen Synthesis in Human Sebocytes. Since HSD3B1 catalyzes the rate-limiting step in the synthesis of sex steroid hormones, we next sought to determine whether sebocytes treated with IL-4 and IL-13 would produce greater amounts of sex steroid hormones. Using liquid chromatography–tandem mass spectrometry (LC-MS/MS), we quantified the amount of sex steroid hormones produced in SZ95 cells in the presence of the precursor dehydroepiandrosterone (DHEA) (Dataset S2). DHEA, which is a substrate of the HSD3B1 enzyme (Fig. 3*A*) and the most abundant androgen in human serum, is greatly reduced with the treatment of IL-4 and IL-13 cytokines (Fig. 3*B*). Furthermore, the amount of androstenedione significantly increased after IL-4 and IL-13 treatment (Fig. 3*B*). The most active androgen in skin is Dihydrotestosterone (DHT), which is the product of the 5-alpha reduction of testosterone. Because DHT is nonpolar, it can be challenging to detect by MS. Therefore, we used a DHT immunoassay of cell culture supernatant and uncovered greater amounts of DHT in sebocytes treated with IL-4 and IL-13 compared to untreated cells (Fig. 3*C*). In sum, these findings show that IL-4 and IL-13 augment sex steroid hormone production in sebaceous gland cells in culture.

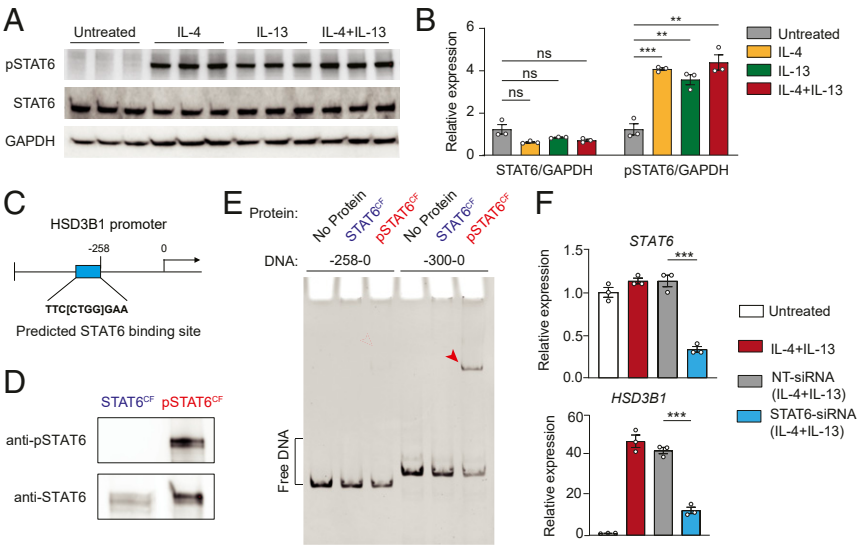

Fig. 2. STAT6 activates *HSD3B1* transcription by binding directly to its promoter. (*A*) Western blot detection of total STAT6 and phosphorylated STAT6 (p-STAT6) in the untreated or IL-4 and IL-13–treated SZ95 cells. GAPDH was used as the loading control. (*B*) Quantification of the Western blot in *A*. Means ± SEM are plotted, $^{**}P < 0.01$, $^{***}P < 0.001$, ns (not significant) was determined by one-way ANOVA. (*C*) Schematic representation of predicted STAT6 binding sites in *HSD3B1* promoter region. (*D*) Western blot analysis was performed using purified $STAT6^{CF}$ (core fragment, amino acids 123 to 658) and $pSTAT6^{CF}$ protein. Human $STAT6^{CF}$ protein was expressed in *E. coli* BL21-CodonPlus (DE3)-RILP cells. $pSTAT6^{CF}$ protein was achieved by coexpressing with an inducible tyrosine kinase gene (pTK) contained in the bacterial strain. (*E*) Electrophoretic mobility shift assay. Purified protein was mixed with indicated fragments of PCR-amplified *HSD3B1* promoter DNA to test for binding ability. $pSTAT6^{CF}$ (−300 to 0)–DNA (300 base pairs long starting at the −1 position) complex has hindered movement in a 6% polyacrylamide DNA retardation gel, which is shown as a shifted band highlighted with the red arrow. (*F*) Relative expression of *STAT6* and *HSD3B1* transcript in SZ95 sebocyte cells treated with IL-4 and IL-13 cytokines ± STAT6-siRNA compared to Nontargeting (NT) control siRNA. Means ± SEM are plotted, $^{**}P < 0.01$, $^{***}P < 0.001$, ns (not significant) was determined by one-way ANOVA.

Given that IL-4 and IL-13 cytokines promote HSD3B1 expression and androgen synthesis in human sebocytes, we next sought to prove that androgen synthesis in sebaceous cells was dependent on HSD3B1 using siRNAs. Transfection of SZ95 sebocytes with *HSD3B1* siRNA reduced HSD3B1 protein expression by 60% compared to a scrambled siRNA negative control (*SI Appendix*, Fig. S6 *A–C*). As predicted, knockdown of *HSD3B1* resulted in significantly decreased androgen production and less consumption of DHEA in comparison with cells transfected with a scrambled control (Fig. 3 *D* and *E*). Furthermore, overexpression of HSD3B1 through transfection of an HSD3B1 expression plasmid (*SI Appendix*, Fig. S6*D*) led to augmented DHT production in cells (*SI Appendix*, Fig. S6*E*). Taken together, these data show that IL-4 and IL-13 promote androgen synthesis in human sebocytes through HSD3B1.

HSD3B1 Drives Lipids Abnormalities in Human Sebocytes. Sebum lipid production in humans has been observed to correlate with androgen production in skin (26, 27). Additionally, sebum lipids function in barrier formation at the skin surface and are dysregulated in AD (28). Thus, we hypothesized that shifts in androgen production caused by IL-4 ad IL-13 might impact the repertoire of lipids in sebocytes and aggravate barrier disruption in AD. We conducted LC-MS/MS lipidomic analysis of SZ95 cells supplemented with DHEA to determine the impact of HSD3B1 on lipid production (Dataset S3). We observe that the amount of total TAGs declined in sebocytes treated with IL-4 and IL-13 (Fig. 4*A*). TAG fatty acids 18:0, 18:1, 18:2, and 20:4 were less abundant in sebocytes treated with cytokines compared to untreated controls (*SI Appendix*, Fig. S7*A*). Interestingly, we also observed greater amounts of diacylglycerides (DAGs) after treatment, suggesting that IL-4 and IL-13 might trigger the breakdown of TAGs to DAGs via lipolysis in sebocytes (Fig. 4*A*).

Next, to determine the requirement of HSD3B1 in lipid production, we transfected sebocytes with siRNA targeting HSD3B1. We observed a robust increase of ~1.76-fold in total TAG as compared with cells transfected with a nontargeting siRNA control (Fig. 4*A*). All detectable fatty acid species present in the sebaceous TAG were significantly increased after knockdown of HSD3B1 (*SI Appendix*, Fig. S7*B*). Additionally, knockdown of HSD3B1 lead to a decrease in the amounts of SMs in human sebocytes (Fig. 4*A*). Across all experimental groups, there were less significant shifts in the amount of cellular membrane lipids, such as phosphatidic acid (PA), and no change in the relative abundance of ceramides (Fig. 4*A* and *SI Appendix*, Fig. S8). Collectively, these results link the regulation of HSD3B1 to changes in TAG production in human sebocytes.

To further probe how augmented sex steroid hormone production in AD might affect lipid synthesis, we quantified the impact of IL-4 and IL-13 combined with DHEA on a set of genes central to cellular lipid metabolism in skin, including diglyceride acyltransferase (DGAT), peroxisome proliferator-activated receptor gamma (PPARG), insulin-induced gene 1 (INSIG1), fatty acid desaturases (FADS), and fatty acid elongases (ELOVL). We observed a more than twofold increase of *INSIG1* expression after IL-4 and IL-13 treatment (Fig. 4*B* and *SI Appendix*, Fig. S7*C*). Overexpression of HSD3B1 also led to an increase in *INSIG1* expression (Fig. 4*C*). Furthermore, siRNA knockdown of HSD3B1 (and the concomitant decrease of androgens) resulted in decreased expression of *INSIG1* (Fig. 4*D*). Based on these findings, we hypothesized that androgens might directly stimulate *INSIG1* expression in sebocytes. We treated SZ95 cells with testosterone and found that testosterone alone could significantly boost the expression of *INSIG1* (Fig. 4*E*).

Lastly, we tested the impact of a loss of androgens on the expression of cellular lipid metabolism in sebocytes through siRNA targeting HSD3B1. Consistent with our findings that HSD3B1-siRNA lead to an increase in the amount of triglyceride (Fig. 4*A*), knockdown of HSD3B1 leads to an increase in a series of enzymes involved in lipid synthesis: *DGAT1*, *DGAT2*, *FADS1*, and *ELOVL1* (Fig. 4*F*). Moreover, keratinocytes

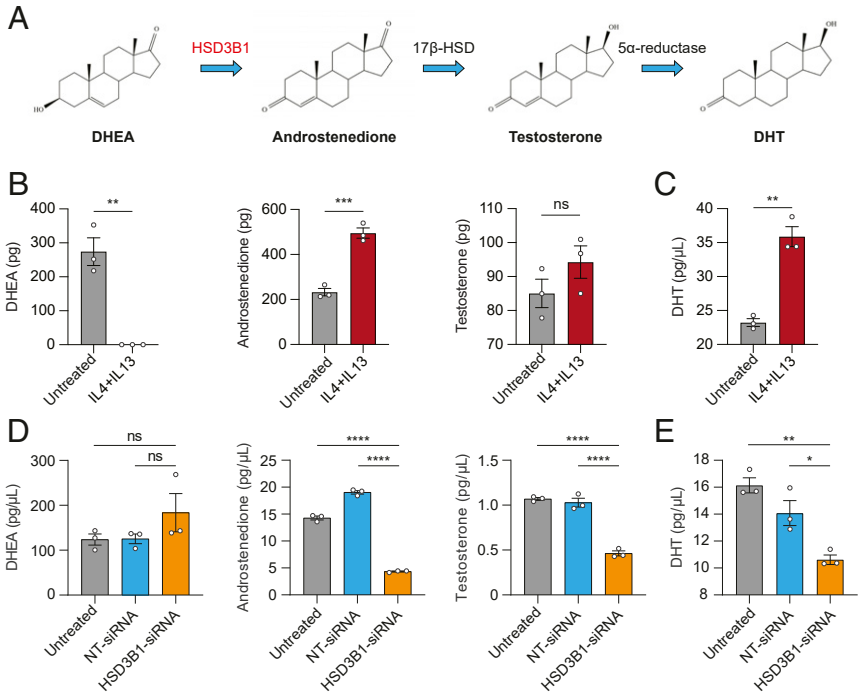

Fig. 3. IL-4 and IL-13 cytokines induce androgen synthesis in human sebaceous gland cells through HSD3B1. (*A*) Schematic representation of the major mammalian androgen synthesis pathway. The enzyme HSD3B1 (highlighted in red) is the rate-limiting step for biosynthesis of all classes of androgens. (*B* and *D*) LC-MS/MS analysis of steroid hormone levels in SZ95 cells (*B*) and culture supernatant (*D*). Cells were treated with IL-4 and IL-13 cytokines (*B*) or transfected with *HSD3B1* siRNA to knockdown *HSD3B1* (*D*). Nontargeting (NT) control siRNA was used as negative control. (*C* and *E*) Enzyme-linked immunosorbent analysis of DHT levels in human sebaceous gland SZ95 cell culture supernatant. Cells were treated with IL-4 and IL-13 cytokines (*C*) or transfected with *HSD3B1* siRNA (*E*). NT control siRNA was used as negative control. The cultured human SZ95 cells were supplemented with 100 nM DHEA as the precursor. Means ± SEM are plotted, $****P < 0.0001$, $***P < 0.001$, $**P < 0.01$, $*P < 0.05$, ns (not significant) was determined by unpaired *t* test (*B* and *C*) or one-way ANOVA (*D* and *E*).

cultured with the supernatant of sebocytes treated with siRNA targeting HSD3B1 also show increased relative expression of the lipid synthesis genes, *PPARG*, *INISG1*, *FADS1*, *FADS2*, and *DGAT1* compared to control (*SI Appendix*, Fig. S9*A*). Conversely, mouse skin treated with the androgen DHT shows lower expression of *Dgat2*, *Elovl1*, *Fads1*, and *Fads2* (*SI Appendix*, Fig. S9*B*). Taken together, our findings demonstrate that regulation of sex steroid hormone synthesis impacts lipid production in skin. Furthermore, IL-4 and -13 may alter skin lipid production in AD through the regulation of sex steroid hormone synthesis in the sebaceous gland (Fig. 4*G*).

Androgen Synthesis Is Enhanced in the MC903-Driven Mouse Model of AD. Given the significant shift of androgen synthesis in human sebocytes, we next set out to examine the possibility of leveraging a murine AD model to elucidate the physiological function of this pathway in AD. We employed an established AD mouse model through the daily topical application of the vitamin D analog MC903 (calcipotriol) (Fig. 5*A*). The MC903 AD mouse model recapitulates key features of AD, including increases in the cytokines IL-4 and IL-13 (Fig. 5*D*). Compared with control mice treated with ethanol (ETOH) only, MC903-treated mice developed robust skin inflammation with histologic features reminiscent of human AD, such as hyperplasia of the epidermis and dermal infiltrate with immune cells (Fig. 5*B* and *SI Appendix*, Fig. S11*B*).

Unlike primates, rodent adrenal glands lack the enzymatic machinery required to synthesize DHEA—the circulating precursor of sex steroid hormones in humans and a key substrate of HSD3B1 (*SI Appendix*, Fig. S2) (29). Noting these differences between mice and humans, we explored the expression of *Hsd3b6* and *Cyp11a1*, the murine homologs of *HSD3B1* and *CYP11A1* (*SI Appendix*, Fig. S10). Consistent with our human sebocyte data (Fig. 1), *Cyp11a1* transcripts are more abundant in the AD mouse model. However, unlike our observation in human skin samples, *Hsd3b6* transcript is expressed at lower amounts in the mouse model of AD compared to control skin (Figs. 5*D* and 1*E*). Our findings were further confirmed by analyzing the RNA-seq data published by Oetjen et al. comparing vehicle and MC903-treated mouse skin (*SI Appendix*, Fig. S11*C*) (30). Notably, bioinformatic analysis of this dataset also revealed the expression of several genes including *Akr1c18* (mouse ortholog of human *AKR1C13*), *Cyp1b1*, and *Hsd17b12* that are differently regulated in the MC903-driven AD mouse model as compared to human AD patients (*SI Appendix*, Fig. S4*C*). Taken together, these data shed light on the known differences between mouse and human endocrinology, while also suggesting that sex steroid hormone biosynthesis could be altered in both species when IL-4 and IL-13 levels are elevated.

Next, using LC-MS/MS analysis for sex steroid hormones, we tested whether MC903 treatment would impact androgen synthesis in mouse skin. Consistent with the reported absence of circulating DHEA in rodents (23), DHEA was not detectable in mouse skin (Dataset S2). However, the amount of androstenedione was significantly increased in MC903-treated mice, in parallel to what we observed in human sebocytes in culture (Figs. 5*C* and 3*B*). Though the mechanism in mice is unclear, our findings show that androgen synthesis is enhanced in the MC903 mouse model of AD.

Lipid Production Is Altered in an MC903-Driven Mouse Model of AD. In sebocytes in culture, the increase in androgens correlated with a decrease in TAG in cells in culture. Furthermore, DHT-treated mouse skin showed decreased expression of lipid synthesis genes

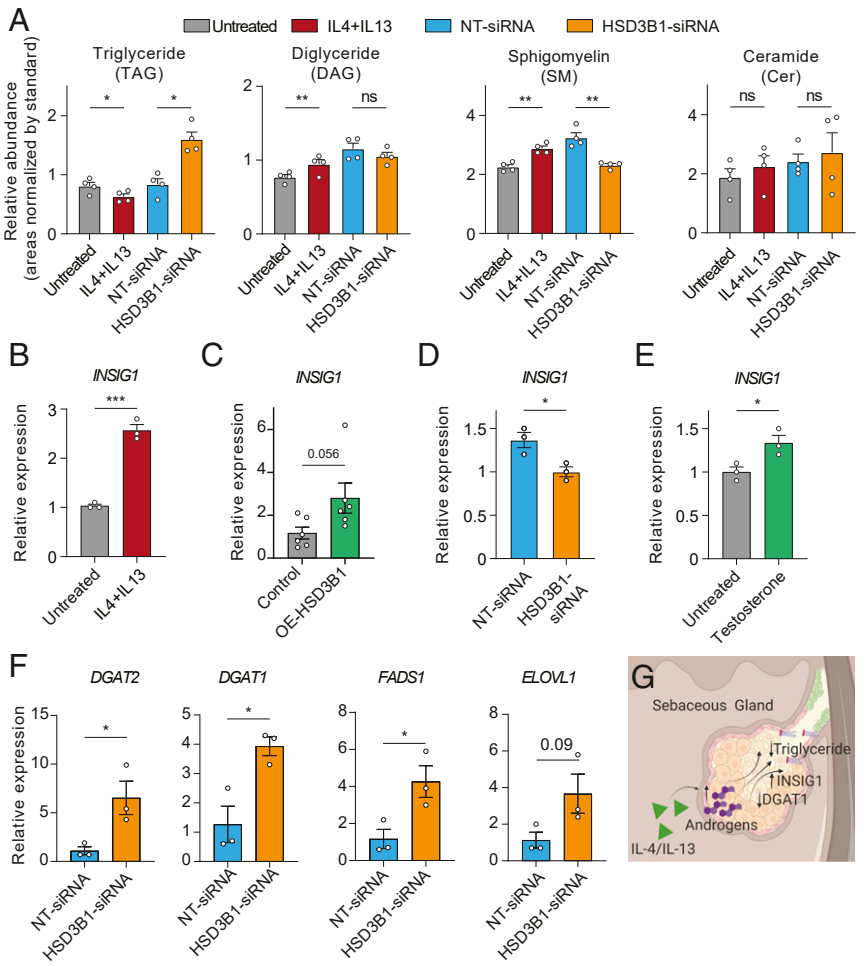

Fig. 4. IL-4 and IL-13–induce lipid abnormalities through HSD3B1. (*A*) LC-MS/MS lipidomic analysis of SZ95 cells treated with IL-4 and IL-13 cytokines or transfected with *HSD3B1* siRNA compared to Nontargeting (NT) control siRNA. The cultured human SZ95 cells were supplemented with 100 nM DHEA as a precursor. Relative abundance of total Triglyceride (TAG), Diglyceride (DAG), Sphingomyelin (SM), and Ceramide (Cer) are plotted as means ± SEM. (*B–E*) Relative expression of *INSIG1* in SZ95 sebocyte cells treated with the following: IL-4 and IL-13 cytokines (*B*), a plasmid overexpressing HSD3B1(*C*), siRNA targeting *HSD3B1* (*D*), or 1 μM testosterone (*E*) compared to control. Knockdown of *HSD3B1* in sebocytes increases the expression of triglyceride synthesis machinery in sebocytes (*F*). Relative expression of *DGAT2, DGAT1*, *FADS1*, and *ELOVL1* in SZ95 sebocytes transfected with *HSD3B1* siRNA compared to NT control siRNA (*F*). IL-4 and IL-13 drive lipid abnormalities in sebocytes through regulation of sex steroid hormone production (*G*). Means ± SEM are plotted, ***$P < 0.001$, **$P < 0.01$, *$P < 0.05$, ns (not significant) was determined by unpaired *t* test.

in skin (*SI Appendix*, Fig. S9*B*). Thus, we predicted that higher amounts of androstenedione in the MC903-AD model would correlate with decrease triglycerides in mouse skin. We performed LC-MS/MS of mouse skin to further characterize changes to lipid species in the AD mouse model (Dataset S4). In parallel to what we observed in cell culture (Fig. 4*A* and *SI Appendix*, Fig. S7*A*), LC-MS/MS data revealed a decrease in the total triglycerides (TAG) in the MC903-driven AD mouse model (Fig. 5*E*). We further analyzed specific fatty acids (FA) present in skin triglycerides. Among them, FA 18:1 and FA 18:2 are most abundant in skin. We observed a reduction of all detected fatty acid species after MC903 treatment (Fig. 5*E*).

Discussion

In this study, we report that rate-limiting enzymes in the sex steroid hormone synthesis pathway, CYP11A1 and HSD3B1, are markedly up-regulated by IL-4 and IL-13 in human sebaceous gland cells (Fig. 1). Using the LC-MS/MS technique, we also demonstrate that elevations in IL-4 and IL-13 correlate with enhanced androgen production and lipid abnormalities in mouse skin and human sebocytes (Figs. 3–5). In human cells, we show mechanistically that IL-4 and IL-13 lead to the phosphorylation of STAT6 in human sebocytes, which activates *HSD3B1* transcription by binding directly to its promoter (Fig. 2). Furthermore, the expression of HSD3B1 is also highly elevated in the lesional skin of AD patients and can be restored by blocking IL-4Rα signaling through Dupilumab treatment (Fig. 1). Taken together, these data demonstrate that IL-4 and IL-13 enhance androgen synthesis in humans through regulation of *HSD3B1*. Furthermore, regulation of *HSD3B1* drives lipid abnormalities in skin (Fig. 4 *E–G*).

While previous studies have successfully established the link between IL-4 and IL-13 and AD pathogenesis (31), our findings highlight a previously unappreciated interaction between the immune system and the epithelium in AD. Specifically, our findings show that IL-4 and IL-13 regulate sex steroid hormone synthesis machinery in skin, leading to enhanced HSD3B1-dependent androgen production and decreased TAG amounts in human sebaceous gland cells. Our data are consistent with prior work indicating that human sebaceous glands express steroidogenic enzymes and that HSD3B1 expression correlates with the concentration of androstenedione in human skin (32, 33).

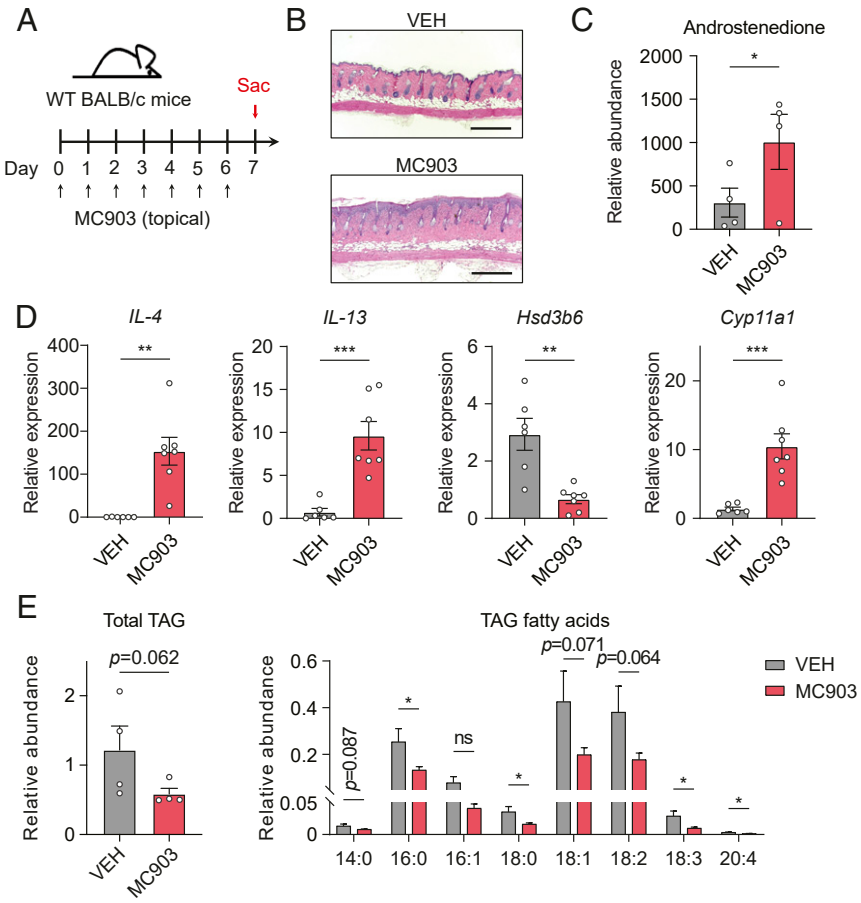

Fig. 5. Androgen synthesis is enhanced, and triglycerides are diminished in the MC903-driven AD mouse model. (*A*) Experimental schematic of the daily topical MC903 treatment-driven AD mouse model. (*B*) Representative hematoxylin & eosin staining of mouse skin treated with MC903 compared to vehicle control. (Scale bar, 500 μm.) (*C*) LC-MS/MS analysis of androstenedione levels in back skin. Mice skin was treated with MC903 or vehicle control. (*D*) Relative expression of *IL-4*, *IL-13*, *Hsd3b6*, and *Cyp11a1* in MC903-treated skin compared to vehicle-treated skin (VEH). $n \geq 4$ mice per group. (*E*) LC-MS/MS lipidomic analysis of MC903-driven AD mice skin compared to vehicle-treated control skin. Relative abundance of total Triglyceride (TAG) and specific TAG fatty acid (FA) are plotted as means ± SEM, $*P < 0.05$, $**P < 0.01$, $***P < 0.001$, ns (not significant) was determined by unpaired *t* test.

Our data innovatively reveal how the immune system modulates sex steroid hormone production in sebocytes and its involvement in AD pathogenesis. Additional studies will be required to determine if patients with AD generate more sex steroid hormone compared to controls, as we show in the mouse AD model (Fig. 5*C*). Our findings that the skin is a local and dynamic source of sex steroid hormones has implications for other peripheral sites such as the lung and the gastrointestinal tract—where IL-4 and IL-13 function in asthma pathogenesis and antihelminth defense. Additional studies using LC-MS/MS analysis and the generation of sebaceous gland-specific mouse models will be required to further elucidate the interplay between the immune system, extragonadal sources of sex steroid hormones, and the skin epithelium.

Our data also reveal a lower amount of total TAG when sebocytes are treated with IL-4 and IL-13 compared to untreated cells. In the skin, TAGs are broken down to FFAs and glycerol that play a critical role in the generation and maintenance of the epidermal permeability barrier (16). Decreased levels of two unsaturated FAs, FA 16:1 and FA 18:1, are observed in atopic skin (3) and correlate with the skin dryness phenotype seen in AD patients. Indeed, decreased TAG at the skin surface is thought to be an initiating event in AD (28, 34). Though changes in key lipid metabolism genes are associated with AD (35), what causes these changes during AD pathogenesis remains incompletely understood. Our results reveal that regulation of androgen production can drive down the amounts of TAG in sebocytes through induction of *INSIG1* expression and repression of the lipid synthesis genes *DGAT2*, *DGAT1*, *FADS1*, and *ELOVL1* (Fig. 4 and *SI Appendix*, Fig. S9). INSIG1 impairs lipogenesis in other cell types. Thus, its upregulation in the setting of increased HSD3B1 expression may underlie the decrease in total TAG observed in our system (36). Furthermore, we demonstrate that knockdown of *HSD3B1* in sebocytes leads to an increase in total triglyceride and increased expression of lipid synthesis machinery in both sebocytes and keratinocytes (Fig. 4*F* and *SI Appendix*, Fig. S9*A*). Taken together, these findings suggest that inhibition of HSD3B1 may boost TAG content in human skin and could have therapeutic potential in AD. Additional studies are needed to further dissect mechanistically how sex steroid hormones regulate lipogenesis in mammalian skin.

Materials and Methods

Ethics. This study was carried out in accordance to the Guide for the Care and Use of Laboratory Animals of University of Texas (UT) Southwestern Medical Center. The mouse protocols were approved by the Institutional Animal Care and Use Committee. This study was approved by the UT Southwestern Institutional Review Board protocols STU-072018-067 and STU-2020-0812. All human subjects provided written informed consent prior to their participation in the study.

Mice. BALB/C wild-type mice were bred and housed in the specific pathogen free barrier facility at the UT Southwestern Medical Center. Naive adult (8 to

12 wk) male mice were used for all experiments. Mice were randomly assigned to treatment groups.

Immunohistochemistry. Human skin samples were fixed in formalin overnight and embedded in paraffin by the UT Southwestern histology core. Samples were deparaffinized in xylene followed by decreasing ethanol rehydration steps followed by epitope retrieval. The slides were incubated with a peroxidase suppressor and a blocking buffer from a commercialized immunohistochemistry kit (36000, ThermoFisher). Samples were then incubated overnight at 4 °C with primary antibodies against HSD3B1 (LS-B10158-50) or mouse IgG isotype control (Thermo Fisher 02-6502) at 1:100 concentration. The secondary antibody, goat anti-mouse IgG secondary antibody conjugated with horseradish peroxidase (HRP) (G-21040, ThermoFisher), was diluted at 1:100 concentrations as well. Visualization was obtained with a DAB/Metal concentrate (10×) diluted in a peroxide buffer. The samples were counterstained with Vector Nuclear Fast Red (NC9483816, ThermoFisher). Images were captured with the Echo Revolve 4 microscope. Human skin was obtained from healthy individuals undergoing plastic surgery at UT Southwestern. AD lesional skin was obtained from additional sections of a paraffin embedded block of a confirmed case of AD.

Immunofluorescence. Samples were deparaffined with xylene followed by rehydration with decreasing concentrations of ethanol. Boiling in 10 mM sodium citrate buffer with 0.2% tween for 15 min was performed for antigen retrieval. Slides were blocked with 10% fetal bovine serum (FBS), 1% bovine serum albumin, and 1% Triton X-100 in phosphate buffered saline for 1 h and then incubated with primary antibodies against HSD3B1 (LS-B10158-50), PLIN2 (Progen GP40), or IgG isotype control (Thermo Fisher 02-6502 and Novus NBP1-97036) using 1:150 dilutions at 4 °C overnight. Secondary antibodies Alexa Fluor 594 or 647 (Thermo Fisher) were diluted 1:350 and applied to slides for 1 h at room temperature in the dark. Slides were then washed with PBST (PBS with 0.2% tween) and mounted with DAPI Fluoromount-G (Southern Biotechnology 0100-20). Images were captured using an Echo Revolve 4 microscope.

Real-time qPCR. RNA was extracted from mouse skin tissue or cultured cells (HaCaT, SEB-1, or SZ95) using the RNAeasy Plus universal kit (Qiagen 73404). RNA was quantified by absorbance at 260 nm, and its purity was evaluated by the ratios of absorbance at 260/280 nm (around 2.0). For complementary DNA (cDNA) synthesis, 2 μg RNA was used (Thermo Fischer 4368814, High Capacity cDNA reverse transcription kit). Real-time qPCR was performed using PowerUp SYBR Green Gene Expression Assays (Thermo Fischer A25741) and the QuantStudio 7 Flex Real-Time PCR System (Applied Biosystems). Relative expression values were determined using the comparative Ct (ΔΔCt) method, and transcript abundances were normalized to GAPDH or 18S transcript abundance. The sequences of the primers are shown in *SI Appendix*, Table S1.

Whole-Transcriptome Sequencing and Data Analysis. RNA was extracted from SZ95 cells using the RNAeasy Plus universal kit (Qiagen 73404). RNA quality was assessed by Agilent 2100 Bioanalyzer. Truseq RNA sample preparation kit version 2 (Illumina) was used for the preparation of sequencing libraries. Sequencing was performed on an Illumina HiSEq. 2500 for signal end 50-base pair length reads. Sequence reads were mapped against the hg19 genome using TopHat. For each gene, read counts were computed using HTSeq-count and analyzed for differential expression using DESeq2 with parameters fold change >1.8 and adjusted *P* value <0.01.

Analysis of RNA-Seq Data. We analyzed the publicly available RNA-seq dataset, PubMed Unique Identifier (PMID): 29467325 (11). Differential gene expression analysis was done using the R package edgeR (version 3.10.5). Genes were selected with Counts Per Million >10 in at least eight samples. Cutoff values of absolute fold change greater than 2.0 and false discovery rate (FDR) ≤0.05 were then used to select for DEGs between sample group comparisons.

Western Blot. Cultured cells were harvested by applying 200 μL diluted 1× sample buffer (Thermo Fisher 39000) directly to a 6-well plate, scraping down the cell sample to disrupt the membranes, then boiling for 15 min before loading. Equal amounts of protein were loaded onto a 4 to 20% gradient sodium dodecyl sulfate–polyacrylamide gel electrophoresis (SDS-PAGE) and transferred to a polyvinylidene fluoride membrane. After blocking with 5% milk in Tris buffered saline with Tween, the membranes were incubated at 4 °C overnight with anti-HSD3B1 antibody (LS-B10158-50), anti-STAT6 (Cell signaling 9362), anti–P-STAT6 (Abcam ab28829), anti-HSP27 (Cell Signaling Technology; 2402S), or anti-GAPDH (Abcam ab181602). Membranes were then incubated with anti-mouse or anti-rabbit secondary antibodies conjugated with HRP (Abcam). Membranes were visualized and bands quantified using a Bio-Rad ChemiDoc Touch system and Image Lab software.

Cell Culture and Treatment. SZ95 (21) and SEB-1 (22) sebocytes were maintained in Sebomed Basal Medium (Fischer Scientific NC9711618) supplemented with 10% fetal bovine serum (GeminiBio 100-106), 5 ng/mL human epidermal growth factor (ThermoFisher PHG0313), and 1% Antibiotic-Antimycotic (Gibco 15240062). HaCaT cells (AddexBio; T0020001) were maintained in opti-Dulbecco's Modified Eagle Medium (AddexBio; C0003-02) with 10% FBS and 1% Antibiotic-Antimycotic solution. Cells were cultured in 37 °C, 5% CO_2 incubator. Cells were stimulated with 10 ng/mL recombinant human cytokines including IL-4, IL-5, IL-13, IL-33, IL-17α, IL-23, or IFN-γ (Biolegend 574002, 560701, 571102, 581802, 570502, 574102, and 570202). After PBS wash, 24-h poststimulation cells were harvested, and RNA extraction was performed as described above for real time qPCR.

Protein Expression and Purification. The gene encoding human $STAT6^{CF}$ (amino acids 123 to 658) was amplified from the human STAT6 (NM_003153) open reading frame (ORF) clone (Origene, RC210065) and was cloned into the pET28(a)+ expression vector. The amplicon was placed between the NdeI and XhoI restriction endonuclease sites with an N-terminal hexa-histidine tag.

In order to obtain the unphosphorylated human $STAT6^{CF}$ protein, proteins were expressed in *E. coli* BL21-CodonPlus (DE3)-RILP cells (Stratagene) by induction with 0.4 mM isopropyl-β-D-galactoside (IPTG) for 12 h at 18 °C. Cells were harvested, resuspended in buffer containing 25 mM Tris HCl pH 8.0 and 150 mM NaCl, and lysed by sonication. After centrifugation at 10,000 *g* for 50 min, the supernatant was loaded onto a Ni^{2+} metal affinity column (Qiagen). Nonspecific contaminants were washed away with buffer containing 25 mM Tris HCl pH 8.0, 150 mM NaCl, and 30 mM imidazole. Protein was eluted in buffer containing 25 mM Tris HCl pH 8.0, 150 mM NaCl, and 300 mM imidazole. The eluate was desalted with a PD-10 desalting column (GE Life Sciences) into the resuspension buffer. The protein was then eluted from the heparin column (GE Life Sciences) with ∼400 mM NaCl and further purified by size exclusion chromatography on a Superdex 200 Increase 10/300 GL column (GE Life Sciences) preequilibrated with 20 mM Hepes pH 7.0, 200 mM NaCl, 0.5 mM EDTA, 10 mM $MgCl_2$, and 4 mM DTT. Fractions containing the protein were pooled and concentrated for further experiments.

In order to obtain the phosphorylated human $STAT6^{CF}$ protein, proteins were expressed in *E. coli* BL21 (DE3) TKB1 strain (Agilent Technology, 200134), and phosphorylation of $STAT6^{CF}$ protein was achieved by coexpressing with an inducible tyrosine kinase gene (pTK) contained in the bacterial strain following the manufacturer's protocol. Briefly, human $STAT6^{CF}$ proteins were expressed in the *E. coli* BL21 (DE3) TKB1 cells in Luria-Bertani (LB) broth supplemented with 0.4 mM IPTG for 12 h at 18 °C. Cells were collected by centrifugation at 2,000 *g* and were then resuspended in the TK induction medium to an optical density at 600 nm (OD_{600}) of 0.5. The TK-induced cultures were further incubated for 2 h at 37 °C with shaking. Phosphorylated human $STAT6^{CF}$ proteins were purified from these cells by Ni^{2+} affinity chromatography, heparin column, and size exclusion chromatography using the same procedures as described for unphosphorylated human $STAT6^{CF}$ proteins.

Electrophoretic Mobility Shift Assay. Purified protein was stored at −80 °C freezer in binding buffer (20 mM Tris HCL, 50 mM NaCl, 40 mM EDTA, 4 mM DTT, 10% glycerol, pH 6.8). PCR-amplified promoter regions of the HSD3B1 gene were purified using the QIAquick PCR Purification kit (Qiagen). Binding reactions of protein to DNA probes were performed in binding buffer mentioned for storage of purified protein above with 0.5 mg/mL BSA, in 25 μL total volume, at 37 °C for 30 min. Reaction mixtures were run in a 6% polyacrylamide DNA retardation gel (Invitrogen) in 0.5 Tris-borate-EDTA (TBE) buffer (Invitrogen) at 160 V for 45 min, and gels were stained with ethidium bromide in 0.5 TBE buffer for 10 min at room temperature before being exposed to ultraviolet light for imaging using the Bio-Rad ChemiDoc Touch system.

Gene Silencing by siRNA. For knockdown studies, SZ95 sebocytes were transfected by addition of transfection mixture containing 10 nM *HSD3B1* or *STAT6* siRNA using Lipofectamine RNAiMax (Invitrogen 13778030), according to manufacturer's instructions. As a control, 10 nM nontargeting control siRNA was transfected in the same procedure. The siRNA constructs were obtained as ON-TARGET plus SMART pool *HSD3B1* (L-008972-00-0005), *STAT6* (L-006690-00-0005), and ON-TARGET plus nontargeting siRNA (D-001810-01-05) from Dharmacon (Horizon Discovery). Cells were incubated for 48 h at 37 °C, and

the efficiency of *HSD3B1* knockdown was evaluated by Western blotting and RT-PCR.

HSD3B1 Overexpression. For HSD3B1 overexpression, 2×10^5/well of SZ95 cells in 6-well plate were seeded for 24 h. A total of 200 ng of either HSD3B1-expressing (Sinobiologicals; HG14410-CH) or control (Sinobiologicals; CV015) plasmids were transfected using Lipofectamine 3000 reagent (Thermo Fisher Scientific; L300015) for 48 h, per manufacture instructions. Cells and supernatants were further analyzed as described.

HaCaT Cells Cultured with SZ95 Supernatant. SZ95 cells were transfected with siRNA targeting HSD3B1 or a nontargeting control in 6-well plate as described. At 48 h posttransfection, the SZ95 culture media was replaced with 2 mL fresh media containing 100 nM DHEA. After 24 h, the supernatants from the respective groups were collected and centrifuged at $400 \times g$ for 5 min and the pellet discarded. Supernatant was then transferred to previously seeded HaCaT cells. After 24 h, HaCaT cells were harvested for RNA isolation and qPCR analysis as described above for real time qPCR.

Sample Preparation for Steroid Hormone and Lipid Analysis. The cultured human SZ95 sebocytes were transfected with siRNA as described above for gene silencing by siRNA. Cells were incubated for 2 d at 37 °C, then supplemented with 100 nM or 1 μM DHEA as the precursor and stimulated with recombinant human cytokines including IL-4 and IL-13 (Biolegend 574002, 571102). At 24 h poststimulation, the supernatant or cell pellets were harvested and snap frozen in liquid nitrogen for steroid hormone or lipid analysis.

Mouse Treatments with MC903 or DHT. The 8-wk-old BALB/c mice were obtained from UT Southwestern mouse breeding core or from The Jackson Laboratory (Stock no. 000651). The dorsal back hair was removed by shaving (Andis ProClip), followed by depilatory cream (Nair). After 24 h, BALB/c mice were topically treated once daily with either 20 μL ethanol alone (vehicle) or with ethanol containing 2 nmol MC903 (calcipotriol, Tocris Bioscience 2700) for 7 d as previously described (37). Similarly, for the DHT study mice were treated daily with 20 μL ethanol alone or with ethanol containing 100 nmol DHT for 7 d on the dorsal back. At the end of the MC903 or DHT treatment, mice were euthanized and murine back skin tissues from the treated site were analyzed by real-time qPCR or harvested and snap frozen in liquid nitrogen for LC-MS/MS analysis. Remaining treated skin tissues were fixed in formalin and embedded in paraffin for histological analysis. All images were captured with an Echo Revolve 4 microscope.

Quantification of Sex Steroid Hormone Levels. Approximately 50 mg skin tissue was used for LC-MS/MS steroid analysis in a method adapted from Peitzsch et al. (38). The skin was added to Omni Bead Ruptor tubes and homogenized in 400 μL H_20. The sample was transferred to Eppendorf tubes, and protein was precipitated out using 200 μL $ZnSO_4$ followed by 400 μL cold MeOH. The deuterated internal standard was added, and the slurry was vortexed and centrifuged at 4,700 rpm for 10 min resulting in a protein pellet. The samples were then taken through a solid phase extraction protocol using Biotage Evolute Express ABN 30 mg/1 mL columns. The columns were conditioned using 1 mL Acetonitrile and 1 mL MeOH followed by 500 μL H_2O. The supernatant from the vortexed samples was loaded over 200 μL H_2O. The columns were washed with 500 μL H_2O and 500 μL of 30% MeOH in H_2O. The steroids were eluted using two washes of 500 μL Acetonitrile and collected into 1.5-mL glass inserts. The samples were dried under nitrogen and redissolved in 200 μL MeOH/H_2O 1:1. The samples were quantified using the linear range of a calibration curve created by serial dilution, and the values were normalized to the initial weight of sample used. Because DHT is hard to ionize and cannot be detect by the above approach, DHT Enzyme-linked immunosorbent assay kit (Eagle, DHT31-K01) was used for detection of DHT level in cell culture supernatant, according to the manufacturer's instructions.

LC-MS/MS Lipid Analysis. Approximately 50 mg skin tissue (weighed accurately) was placed in 2-mL microtubes with 2.8-mm ceramic beads, and 1 mL 1:2 (volume [vol]/vol) methanol:dichloromethane was added. Samples were homogenized for five cycles at 5.5 revolutions per second for 10 s for a total of 50 s using an Omni Beadruptor 24. Skin tissue homogenates were transferred to glass tubes and samples were diluted to a concentration of 10 mg/mL with 1:2 (vol/vol) methanol:dichloromethane.

Aliquots equivalent to 250,000 SZ95 cells or 0.5 mg homogenized skin tissue were transferred to fresh glass tubes for liquid–liquid extraction. Samples were dried under N_2 and extracted by modified Bligh/Dyer; 1 mL each of dichloromethane, methanol, and water were added to a glass tube containing the sample. The mixture was vortexed and centrifuged at $2,671 \times g$ for 5 min, resulting in two distinct liquid phases. The organic phase was collected to a fresh glass tube with a Pasteur pipette and dried under N_2. Samples were resuspended in 400 μL Hexane containing 20 μL/mL of 3:50 diluted SPLASH LipidoMix internal standard.

Lipids were analyzed by LC-MS/MS using a SCIEX QTRAP 6500$^+$ equipped with a Shimadzu LC-30AD (Kyoto, Japan) high performance liquid chromatography system and a 150 × 2.1 mm, 5 μm Supelco Ascentis silica column (Bellefonte, PA, USA). Samples were injected at a flow rate of 0.3 mL/min at 2.5% Solvent B (methyl tert-butyl ether) and 97.5% Solvent A (hexane). Solvent B is increased to 5% during 3 min and then to 60% over 6 min. Solvent B is decreased to 0% during 30 seconds while Solvent C (90:10 [vol/vol] Isopropanol-water) is set at 20% and increased to 40% during the following 11 min. Solvent C is increased to 44% for 6 min and then to 60% during 50 seconds. The system was held at 60% of Solvent C during 1 min prior to reequilibration at 2.5% of Solvent B for 5 min at a 1.2 mL/min flow rate. Solvent D (95:5 [vol/vol] Acetonitrile-water with 10 mM Ammonium acetate) was infused postcolumn at 0.03 mL/min. Column oven temperature was 25 °C. Data were acquired in positive and negative ionization mode using multiple reaction monitoring. The LC-MS data were analyzed using MultiQuant software (SCIEX).

Statistical Methods. Data represent mean ± SEM. No method was used to predetermine sample size. Formal randomization techniques were not used; however, mice were allocated to experiments randomly and samples processed in an arbitrary order. All statistical analyses were performed with GraphPad Prism software. To assess the statistical significance of a difference between two treatments, we used Student's *t* tests. To assess the statistical significance of differences between more than two treatments, we used one-way ANOVAs. For all tests, *P* values lower than 0.05 were considered statistically significant. Statistical details of experiments can be found in the figure legends, including how significance was defined and the statistical methods used.

Data Availability. Summary of RNA-seq data are included in the supplemental datasets of this manuscript. All study data are included in the article and/or supporting information.

ACKNOWLEDGMENTS. SEB-1 cells were obtained from Amanda Nelson Ph.D. and Dianne Thiboutot MD. We thank Trevor Hall for his assistance in the studies in SEB-1 cells. T.A.H.-T. was supported by a Harold Amos Award through the Robert Wood Johnson Foundation, a UT Southwestern Disease Oriented Clinical Scholars Program award, and a Burroughs Wellcome Fund Career Award for Medical Scientists. J.G.M. is supported in part by an NIH HL20948. We thank Zheng Kuang and the bioinformatics core facility (BICF) for their help with analysis of RNA-seq data. BICF was supported by a grant from the Cancer Prevention & Research Institute of Texas (RP150596). Fig. 4*G* and *SI Appendix*, Fig. S4*A* were created with Biorender.

1. P. M. Brunner, D. Y. M. Leung, E. Guttman-Yassky, Immunologic, microbial, and epithelial interactions in atopic dermatitis. *Ann. Allergy Asthma Immunol.* **120**, 34–41 (2018).
2. T. Werfel *et al.*, Cellular and molecular immunologic mechanisms in patients with atopic dermatitis. *J. Allergy Clin. Immunol.* **138**, 336–349 (2016).
3. S. Li *et al.*, Altered composition of epidermal lipids correlates with Staphylococcus aureus colonization status in atopic dermatitis. *Br. J. Dermatol.* **177**, e125–e127 (2017).
4. S. C. Dharmage *et al.*, Atopic dermatitis and the atopic march revisited. *Allergy* **69**, 17–27 (2014).
5. S. R. Feldman *et al.*, The challenge of managing atopic dermatitis in the United States. *Am. Heal. Drug Benefits* **12**, 83–93(2019).
6. A. M. Drucker *et al.*, The burden of atopic dermatitis: Summary of a report for the National Eczema Association. *J. Invest. Dermatol.* **137**, 26–30 (2017).
7. E. B. Brandt, U. Sivaprasad, Th2 cytokines and atopic dermatitis. *J. Clin. Cell. Immunol.* **2**, 1–24 (2011).
8. N. A. Gandhi *et al.*, Targeting key proximal drivers of type 2 inflammation in disease. *Nat. Rev. Drug Discov.* **15**, 35–50 (2016).
9. M. D. Howell *et al.*, Cytokine modulation of atopic dermatitis filaggrin skin expression. *J. Allergy Clin. Immunol.* **124** (3, suppl. 2), R7–R12 (2009).
10. B. E. Kim, D. Y. M. Leung, M. Boguniewicz, M. D. Howell, Loricrin and involucrin expression is down-regulated by Th2 cytokines through STAT-6. *Clin. Immunol.* **126**, 332–337 (2008).
11. E. Berdyshev *et al.*, Lipid abnormalities in atopic skin are driven by type 2 cytokines. *JCI Insight* **3**, e98006 (2018).
12. C. Niemann, V. Horsley, Development and homeostasis of the sebaceous gland. *Semin. Cell Dev. Biol.* **23**, 928–936 (2012).

13. H. Fischer *et al*., Holocrine secretion of sebum is a unique DNase2-dependent mode of programmed cell death. *J. Invest. Dermatol.* **137**, 587–594 (2017).
14. M. Lovászi, A. Szegedi, C. C. Zouboulis, D. Törőcsik, Sebaceous-immunobiology is orchestrated by sebum lipids. *Dermatoendocrinol* **9**, e1375636 (2017).
15. T. A. Harris *et al*., Resistin-like molecule a provides vitamin-A- dependent antimicrobial protection in the skin article resistin-like molecule a provides vitamin-A-dependent antimicrobial. *Cell Host Microbe* **25**, 1–12 (2019).
16. N. Bhattacharya, W. J. Sato, A. Kelly, G. Ganguli-Indra, A. K. Indra, Epidermal lipids: Key mediators of atopic dermatitis pathogenesis. *Trends Mol. Med.* **25**, 551–562 (2019).
17. K. Agrawal *et al*., Effects of atopic dermatitis and gender on sebum lipid mediator and fatty acid profiles. *Prostaglandins Leukot. Essent. Fatty Acids* **134**, 7–16 (2018).
18. G. Wu *et al*., Variant allele of HSD3B1 increases progression to castration-resistant prostate cancer. *Prostate* **75**, 777–782 (2015).
19. J. Simard *et al*., Molecular biology of the 3β-hydroxysteroid dehydrogenase/delta5-delta4 isomerase gene family. *Endocr. Rev.* **26**, 525–582 (2005).
20. M. R. Mack *et al*., Blood natural killer cell deficiency reveals an immunotherapy strategy for atopic dermatitis. *Sci. Transl. Med.* **12**, eaay1005 (2020).
21. C. C. Zouboulis, H. Seltmann, H. Neitzel, C. E. Orfanos, Establishment and characterization of an immortalized human sebaceous gland cell line (SZ95). *J. Invest. Dermatol.* **113**, 1011–1020 (1999).
22. D. Thiboutot *et al*., Human skin is a steroidogenic tissue: Steroidogenic enzymes and cofactors are expressed in epidermis, normal sebocytes, and an immortalized sebocyte cell line (SEB-1). *J. Invest. Dermatol.* **120**, 905–914 (2003).
23. S. Gingras, R. Moriggl, B. Groner, J. Simard, Induction of 3β-hydroxysteroid dehydrogenase/delta5-delta4 isomerase type 1 gene transcription in human breast cancer cell lines and in normal mammary epithelial cells by interleukin-4 and interleukin-13. *Mol. Endocrinol.* **13**, 66–81 (1999).
24. A. Azmahani *et al*., Steroidogenic enzymes, their related transcription factors and nuclear receptors in human sebaceous glands under normal and pathological conditions. *J. Steroid Biochem. Mol. Biol.* **144** (Pt B), 268–279 (2014).
25. E. Guttman-Yassky *et al*., Dupilumab progressively improves systemic and cutaneous abnormalities in patients with atopic dermatitis. *J. Allergy Clin. Immunol.* **143**, 155–172 (2019).
26. D. T. Downing, M. E. Stewart, J. S. Strauss, Changes in sebum secretion and the sebaceous gland. *Dermatol. Clin.* **4**, 419–423 (1986).
27. C. Barrault *et al*., Androgens induce sebaceous differentiation in sebocyte cells expressing a stable functional androgen receptor. *J. Steroid Biochem. Mol. Biol.* **152**, 34–44 (2015).
28. E. Proksch, J. M. Jensen, P. M. Elias, Skin lipids and epidermal differentiation in atopic dermatitis. *Clin. Dermatol.* **21**, 134–144 (2003).
29. V. Luu-The, F. Labrie, The intracrine sex steroid biosynthesis pathways. *Prog. Brain Res.* **181**, 177–192 (2010).
30. L. K. Oetjen *et al*., Sensory neurons co-opt classical immune signaling pathways to mediate chronic itch. *Cell* **171**, 217–228.e13 (2017).
31. N. A. Gandhi, G. Pirozzi, N. M. H. Graham, Commonality of the IL-4/IL-13 pathway in atopic diseases. *Expert Rev. Clin. Immunol.* **13**, 425–437 (2017).
32. T. Inoue *et al*., Expression of steroidogenic enzymes in human sebaceous glands. *J. Endocrinol.* **222**, 301–312 (2014).
33. M. Fritsch, C. E. Orfanos, C. C. Zouboulis, Sebocytes are the key regulators of androgen homeostasis in human skin. *J. Invest. Dermatol.* **116**, 793–800 (2001).
34. B. E. Kim, D. Y. M. Leung, Significance of skin barrier dysfunction in atopic dermatitis. *Allergy Asthma Immunol. Res.* **10**, 207–215 (2018).
35. M. Danso *et al*., Altered expression of epidermal lipid bio-synthesis enzymes in atopic dermatitis skin is accompanied by changes in stratum corneum lipid composition. *J. Dermatol. Sci.* **88**, 57–66 (2017).
36. J. Li, K. Takaishi, W. Cook, S. K. McCorkle, R. H. Unger, Insig-1 "brakes" lipogenesis in adipocytes and inhibits differentiation of preadipocytes. *Proc. Natl. Acad. Sci. U.S.A.* **100**, 9476–9481 (2003).
37. B. S. Kim *et al*., TSLP elicits IL-33-independent innate lymphoid cell responses to promote skin inflammation. *Sci. Transl. Med.* **5**, 170ra16 (2013).
38. M. Peitzsch *et al*., An LC-MS/MS method for steroid profiling during adrenal venous sampling for investigation of primary aldosteronism. *J. Steroid Biochem. Mol. Biol.* **145**, 75–84 (2015).